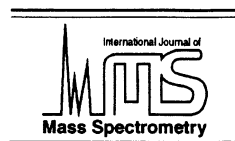




ELSEVIER

International Journal of Mass Spectrometry 181 (1998) 11–25



Structures and energies of C_nS ($1 \leq n \leq 20$) sulphur carbide clusters

G. Pascoli^{a,*}, H. Lavendy^b

^aFaculté des Sciences, Département de Physique, 33 rue Saint Leu, Amiens 80039 Cedex, France

^bLaboratoire de Dynamique Moléculaire et Photonique, CNRS (URA 779), Centre d'Etudes et de Recherches Lasers et Applications Université de Lille1, Bat P5, 59655 Villeneuve d'Ascq Cedex, France

Received 7 May 1998; accepted 3 August 1998

Abstract

C_nS ($1 \leq n \leq 20$) clusters have been investigated by means of the density functional theory. As a general rule, when $1 \leq n \leq 17$ the energetically most favorable isomers are found to be the linear arrangement of nuclei ($C_{\infty v}$) with the sulphur atom at the very end of the carbon chain. The electronic ground state is alternately predicted to be $^1\Sigma^+$ for odd n or $^3\Sigma^-$ for even n with a conspicuous odd–even effect in the stability of these clusters. The $C_{18}S$ cluster is predicted to have a S-capped monocyclic structure (1A_1), but with a low barrier to linearity. On the other hand, $C_{19}S$ and $C_{20}S$ are unambiguously linear in the $^1\Sigma^+$ and $^3\Sigma^-$ electronic ground states, respectively. (Int J Mass Spectrom 181 (1998) 11–25) © 1998 Elsevier Science B.V.

Keywords: Carbon; Clusters; Sulphur carbide; Density functional theory

1. Introduction

In recent years there has been increasing interest in small carbon clusters mixed with heteroatoms. This effort toward understanding the basic principles governing these structures results from the fact that substitutions of heteroatoms (N, Si, S, ...) into a pure carbon cluster is expected to induce significant changes on the electronic structure and the possibilities of new types of materials, with novel solid-state properties [1,2]. Heteroatom-containing carbon clusters has been also identified in space [3] and the way carbon atoms organize into clusters with one or two

heteroatoms is very important in interstellar chemistry [4]. Silicon-substituted carbon clusters have been extensively considered in the literature (see Refs. [5,6]). By comparison, much less information is available for the sulphur carbide clusters even though the fractional abundances of silicon and sulphur are very similar in the interstellar medium, i.e. of the order of 3×10^{-5} and 2×10^{-5} , respectively. Following laboratory microwave spectroscopy, the C_2S and C_3S radicals have been identified in various interstellar media [7–9]. The C_5S species seems to have been also identified in the carbon-rich circumstellar envelope IRC +10 216 [10]. Moreover, the high abundance of C_2S and C_3S suggests that the sulphur chemistry is closely related to the carbon chain chemistry in the interstellar medium [11,12]. Ab

* Corresponding author.

initio calculations have been performed for C_2S and C_3S [13–17] and Lee [18] has more recently calculated the structural parameters, the rotational constants and vibrational frequencies of the linear C_nS compounds up to $n = 9$ using a density functional theory (DFT) method. In the present work, we report an investigation of large sulphur-doped carbon clusters ($C_{1–20}S$) using the density functional theory for which good confidence is expected for medium-sized carbon clusters at moderate cost [6,18–20]. A comparative analysis with pure and silicon-doped carbon clusters is also made. Our main conclusion is that whereas the latter ones (C_n or C_nSi) are found to be linear or cyclic in their ground state when $n < 10$ and cyclic as soon as $n \geq 10$, the C_nS clusters remain linear up to $n = 17$, with a remarkable, and very regular, alternation between singlet or triplet electronic ground states for odd n or even n , respectively. For $n = 18$, the most stable geometry is the S-capped monocyclic ring, while $C_{19}S$ and $C_{20}S$ are again linear.

2. Computational details

We have performed the calculations using the hybrid density functional Kohn–Sham method [21]. The effect of exchange and correlation are approximated by the B3LYP hybrid density functional which is a combination of the three parameter Becke exchange correlation functional [22,23] with the Lee–Yang–Parr nonlocal correlation functional [24]. The Pople's 6-311G* basis set [25] was used for $n \leq 13$. When $n > 13$, the CPU time was largely prohibitive with this basis and the structure was optimized with the standard 6-31G* basis set. From prior experience the use of these basis sets in conjunction with density functional methods leads to quantitatively good results, for pure and heteroatom-containing carbon clusters, especially concerning the structural parameters, the rotational constants and the vibrational frequencies [5,6]. Geometries have been optimized with analytic gradient techniques. Dipole moments have been calculated with the origin at the center of mass and normal modes of vibration with the fully analytic

second derivatives. All the calculations were performed with the GAUSSIAN 94 DFT series of program [26] running on the IBM RS 6000 and the CRAY C94 and C98 of the National Computer Centre Idris in Orsay (France).

3. Results and discussion

Tables 1(a) and 2(a) list the electronic configurations, the energies and the dipole moments of the low-lying (linear and cyclic) structures in both singlet and triplet electronic states. All these quantities are respectively calculated with the 6-311G* basis set when $1 \leq n \leq 13$ and the 6-31G* basis set for $n \leq 13$.

The corresponding optimized structures are graphically displayed in Fig. 1. In Fig. 1 are also reported the structural parameters (distances in angstroms and angles in degrees) and the Mulliken atomic charges (given in parentheses in electronic charge unit/e) for $n \leq 5$. For $n > 5$, these parameters are collected in Tables 1(b) and 2(b). Harmonic vibrational frequencies (in 1/cm), zero-point-energies (in kilocalories per mol) and rotational constants (in gigahertz) are likewise, respectively listed in Tables 5 and 6. These quantities might be very helpful in an experimental (or observational) search in the infrared, millimeter and submillimeter spectra of such clusters. The C_nS ($n \leq 3$) clusters have been extensively discussed elsewhere [13–17] and will not be reconsidered here. By contrast, there have been only a few attempts to study large C_nS clusters ($n \geq 4$) except the theoretical calculations performed by Lee on the linear species $1 \leq n \leq 9$ [18]. In the present study, we restrict ourselves to a discussion of the global properties of these compounds, especially with regard to pure and silicon-doped C_n clusters for which much more information exists in the literature.

The lowest-energy structure for the C_nS clusters is predicted to be the linear arrangement of nuclei when $1 \leq n \leq 17$, in the $^1\Sigma^+$ and $^3\Sigma^-$ electronic ground states, respectively, for odd n and even n . The length of the SC bonds in the n -odd linear isomers varies in an uniform manner along the series from 1.54 Å for

Table 1(a)

Valence orbital configurations, total energies (in hartree), relative stabilities ΔE (in kcal mol⁻¹) and dipole moments (in debye) of the different C_nS ($1 \leq n \leq 13$) structures obtained with a DFT/B3LYP/6-311G* method. The symmetry (point group) and the electronic state of the different structures are also given

Isomer	Point group	State	Electronic configuration	ΔE^a	μ
CS					
lin1 ^b	$C_{\infty v}$	$^1\Sigma^+$	core(σ) ² (σ) ² (π) ² (π) ² (σ) ²	-436.246 153	
lin1'	$C_{\infty v}$	$^3\Pi$	core(σ) ² (σ) ² (π) ² (π) ² (σ) ¹ (π) ¹	0.0	1.84
C ₂ S				-76.9	0.05
lin2	$C_{\infty v}$	$^1\Delta$	core(σ) ² (σ) ² (σ) ² (π) ² (σ) ² (π) ²	-474.272 651	
lin2'	$C_{\infty v}$	$^3\Sigma^-$	core(σ) ² (σ) ² (σ) ² (π) ² (σ) ² (π) ¹ (σ) ¹	20.2	2.64
cyc2	C_{2v}	1A_1	core(a_1) ² (a_1) ² (b_2) ² (b_1) ² (a_1) ² (a_1) ² (b_2) ²	0.0	2.88
cyc2'	C_{2v}	3A_2	core(a_1) ² (a_1) ² (b_2) ² (b_1) ² (a_1) ² (a_1) ² (b_2) ¹ (b_1) ¹	33.3	2.32
C ₃ S				39.6	1.77
lin3	$C_{\infty v}$	$^1\Sigma^+$	core(σ) ² (σ) ² (σ) ² (σ) ² (π) ² (σ) ² (π) ² (σ) ² (π) ²	-512.402 605	
lin3'	$C_{\infty v}$	$^3\Pi$	core(σ) ² (σ) ² (σ) ² (σ) ² (π) ² (σ) ¹ (π) ² (π) ² (π) ¹	0.0	3.50
cyc3	C_{2v}	1A_1	core(a_1) ² (a_1) ² (b_2) ² (a_1) ² (b_1) ² (a_1) ² (b_2) ² (a_1) ¹ (b_1) ¹	59.4	0.67
cyc3'	C_{2v}	3B_2	core(a_1) ² (a_1) ² (b_2) ² (a_1) ² (b_1) ² (b_2) ² (a_1) ² (b_1) ² (a_1) ¹ (b_2) ¹	65.5	3.10
S-cyc3	C_{2v}	1A_1	core(a_1) ² (a_1) ² (a_1) ² (b_2) ² (a_1) ² (b_1) ² (b_2) ² (b_1) ² (a_1) ²	106.2	0.34
S-cyc3'	C_{2v}	3B_2	core(a_1) ² (a_1) ² (a_1) ² (b_2) ² (a_1) ² (b_1) ² (b_2) ² (a_1) ¹ (b_2) ¹	32.6	1.38
C ₄ S				64.6	0.36
lin4	$C_{\infty v}$	$^1\Delta$	core(σ) ² (σ) ² (σ) ² (σ) ² (π) ² (σ) ² (π) ² (σ) ² (π) ²	-550.456 385	
lin4'	$C_{\infty v}$	$^3\Sigma^-$	core(σ) ² (σ) ² (σ) ² (σ) ² (π) ² (σ) ² (π) ² (σ) ² (π) ¹ (π) ¹	14.1	3.78
cyc4	C_{2v}	1A_1	core(a_1) ² (b_2) ² (a_1) ² (b_2) ² (a_1) ² (b_1) ² (a_1) ² (b_2) ² (a_2) ² (b_2) ²	0.0	4.03
cyc4'	C_{2v}	3B_2	core(a_1) ² (b_2) ² (a_1) ² (b_2) ² (a_1) ² (b_1) ² (a_1) ² (b_2) ² (a_2) ² (b_1) ¹ (a_1) ¹	153.6	0.09
S-bicycC4	C_{2v}	1A_1	core(a_1) ² (a_1) ² (a_1) ² (b_2) ² (a_1) ² (b_1) ² (b_2) ² (a_1) ² (b_2) ² (a_1) ²	94.9	0.24
S-bicycC4'	C_{2v}	3A_2	core(a_1) ² (a_1) ² (a_1) ² (b_2) ² (a_1) ² (b_1) ² (b_2) ² (a_1) ² (b_2) ² (a_1) ¹ (b_1) ¹	31.9	1.83
C ₅ S				75.8	4.24
lin5	$C_{\infty v}$	$^1\Sigma^+$	core(σ) ² (π) ²	-588.574 265	
lin5'	$C_{\infty v}$	$^3\Sigma^-$	core(σ) ² (π) ² (σ) ² (π) ² (σ) ² (π) ² (σ) ¹ (π) ¹	0.0	4.65
cyc5	C_{2v}	1A_1	core(a_1) ² (a_1) ² (b_2) ² (a_1) ² (b_2) ² (a_1) ² (b_1) ² (a_1) ² (b_2) ² (a_2) ² (b_2) ² (a_1) ²	47.8	4.23
cyc5'	C_{2v}	3A_2	core(a_1) ² (a_1) ² (b_2) ² (a_1) ² (b_2) ² (a_1) ² (b_1) ² (a_1) ² (b_2) ² (a_2) ² (b_2) ¹ (a_1) ²	54.0	0.68
SC-bicycC4	C_{2v}	1A_1	core(a_1) ² (a_1) ² (a_1) ² (b_2) ² (a_1) ² (b_1) ² (b_2) ² (b_1) ² (a_1) ² (b_2) ² (a_1) ² (b_1) ²	112.0	0.65
SC-bicycC4'	C_{2v}	3A_2	core(a_1) ² (a_1) ² (a_1) ² (b_2) ² (a_1) ² (b_1) ² (b_2) ² (b_1) ² (b_2) ² (a_1) ² (b_1) ¹ (b_2) ¹	58.2	4.05
S-bicycC5	C_{2v}	1A_1	core(a_1) ² (a_1) ² (a_1) ² (b_2) ² (a_1) ² (b_1) ² (b_2) ² (b_1) ² (a_1) ² (b_2) ² (a_1) ² (b_1) ²	87.6	2.93
S-bicycC5'	C_{2v}	3A_2	core(a_1) ² (a_1) ² (a_1) ² (b_2) ² (a_1) ² (b_1) ² (b_2) ² (b_1) ² (a_1) ² (b_2) ² (a_1) ² (b_1) ²	148.9	0.70
C ₆ S				145.8	1.06
lin6	$C_{\infty v}$	$^1\Delta$	core(σ) ² (π) ²	-626.637 877	
lin6'	$C_{\infty v}$	$^3\Sigma^-$	core(σ) ² (π) ¹ (π) ¹	11.1	4.77
cyc6	C_{2v}	1A_1	core(a_1) ² (a_1) ² (b_2) ² (a_1) ² (b_2) ² (a_1) ² (b_2) ² (a_1) ² (b_1) ² (a_1) ² (b_2) ² (a_2) ² (b_2) ² (a_1) ²	0.0	5.04
cyc6'	C_{2v}	3A_2	core(a_1) ² (a_1) ² (b_2) ² (a_1) ² (b_2) ² (a_1) ² (b_2) ² (a_1) ² (b_1) ² (a_1) ² (b_2) ² (a_2) ² (b_2) ¹ (a_1) ²	161.4	0.93
C ₇ S				159.5	0.93
lin7	$C_{\infty v}$	$^1\Sigma^+$	core(σ) ² (π) ²	-664.748 297	
lin7'	$C_{\infty v}$	$^3\Sigma^-$	core(σ) ² (π) ¹ (π) ¹	36.9	5.14
cyc7	C_{2v}	1A_1	core(a_1) ² (a_1) ² (b_2) ² (a_1) ² (b_2) ² (a_1) ² (b_2) ² (a_1) ² (b_1) ² (a_1) ² (b_2) ² (a_2) ² (b_2) ² (a_1) ²	96.0	0.41
cyc7'	C_{2v}	3A_2	core(a_1) ² (a_1) ² (b_2) ² (a_1) ² (b_2) ² (a_1) ² (b_2) ² (a_1) ² (b_1) ² (a_1) ² (b_2) ² (a_2) ² (b_2) ¹ (a_1) ¹	83.9	0.94

(continued)

Table 1(a) (continued)

Isomer	Point group	State	Electronic configuration	ΔE^a	μ
C ₈ S				-702.817 769	
lin8	$C_{\infty v}$	¹ Δ	core(σ) ² (π) ² (π) ² (π) ² (π) ² (σ) ² (π) ² (π) ² (π) ²	9.2	5.73
lin8'	$C_{\infty v}$	³ Σ^-	core(σ) ² (π) ² (π) ² (π) ² (π) ² (σ) ² (π) ² (π) ² (π) ¹ (π) ¹	0.0	6.03
cyc8	C_{2v}	¹ A_1	core(a_1) ² (a_1) ² (b_2) ² (b_1) ² (a_1) ² (a_1) ² (a_2) ² (b_1) ² (a_1) ² (b_2) ² (a_2) ²	101.4	1.37
cyc8'	C_{2v}	³ A_2	core(a_1) ² (a_1) ² (b_2) ² (b_1) ² (a_1) ² (b_1) ² (a_1) ² (a_2) ² (b_1) ² (a_1) ² (b_2) ² (a_2) ¹ (a_1) ¹	121.6	1.04
C ₉ S				-740.923 466	
lin9	$C_{\infty v}$	¹ Σ^+	core(σ) ² (π) ² (π) ² (π) ² (π) ² (π) ² (π) ² (π) ² (σ) ² (π) ²	0.0	6.81
lin9'	$C_{\infty v}$	³ Σ^-	core(σ) ² (π) ² (π) ² (π) ² (π) ² (π) ² (π) ² (σ) ² (π) ² (π) ¹ (π) ¹	27.3	6.21
cyc9	C_{2v}	¹ A_1	core(a_1) ² (a_1) ² (b_2) ² (a_1) ² (b_2) ² (a_1) ² (b_2) ² (a_1) ² (b_1) ² (a_1) ² (b_2) ² (b_1) ² (a_2) ² (a_1) ² (b_2) ² (b_1) ² (a_1) ² (a_2) ² (a_1) ²	100.7	2.71
cyc9'	C_{2v}	³ B_1	core(a_1) ² (a_1) ² (b_2) ² (a_1) ² (b_2) ² (a_1) ² (b_2) ² (a_1) ² (b_1) ² (a_1) ² (b_2) ² (b_1) ² (a_2) ² (a_1) ² (b_2) ² (b_1) ² (a_1) ² (a_2) ² (a_1) ¹ (b_1) ¹	107.4	2.29
C ₁₀ S				-778.996 855	
lin10	$C_{\infty v}$	¹ Δ	core(σ) ² (π) ² (π) ² (π) ² (π) ² (π) ² (π) ² (π) ² (σ) ² (π) ² (π) ²	7.9	6.69
lin10'	$C_{\infty v}$	³ Σ^-	core(σ) ² (π) ² (π) ² (π) ² (π) ² (π) ² (π) ² (π) ² (σ) ² (π) ² (π) ¹ (π) ¹	0.0	7.03
cyc10	C_{2v}	¹ A_1	core(a_1) ² (a_1) ² (b_2) ² (a_1) ² (b_2) ² (a_1) ² (b_2) ² (a_1) ² (b_1) ² (a_1) ² (b_1) ² (b_1) ² (b_2) ² (a_1) ² (a_2) ² (b_2) ² (b_1) ² (a_1) ² (a_2) ² (b_2) ² (b_1) ²	22.9	0.48
cyc10'	C_{2v}	³ B_2	core(a_1) ² (a_1) ² (b_2) ² (a_1) ² (b_1) ² (a_1) ² (b_1) ² (b_2) ² (a_1) ² (a_2) ² (b_2) ² (b_1) ² (a_1) ² (a_2) ² (b_2) ² (b_1) ² (a_1) ¹	54.7	0.43
C ₁₁ S				-817.099 291	
lin11	$C_{\infty v}$	¹ Σ^+	core(σ) ² (π) ² (π) ² (π) ² (π) ² (π) ² (π) ² (π) ² (π) ² (σ) ² (π) ² (π) ²	0.0	7.86
lin11'	$C_{\infty v}$	³ Σ^-	core(σ) ² (π) ² (π) ² (π) ² (π) ² (π) ² (π) ² (π) ² (π) ² (σ) ² (π) ² (π) ¹ (π) ¹	22.9	7.12
cyc11	C_{2v}	¹ A_1	core(a_1) ² (a_1) ² (b_2) ² (a_1) ² (b_1) ² (a_1) ² (b_1) ² (a_1) ² (b_2) ² (a_2) ² (b_2) ² (b_1) ² (a_1) ² (a_2) ² (b_2) ² (b_1) ²	33.7	0.79
cyc11'	C_{2v}	³ A_2	core(a_1) ² (a_1) ² (b_2) ² (b_1) ² (a_1) ² (b_1) ² (a_1) ² (b_2) ² (a_2) ² (b_2) ² (b_1) ² (a_1) ² (a_2) ² (b_2) ² (b_1) ² (a_1) ²	55.9	0.54
C ₁₂ S				-855.175 468	
lin12	$C_{\infty v}$	¹ Δ	core(σ) ² (π) ² (π) ² (π) ² (π) ² (π) ² (π) ² (π) ² (π) ² (σ) ² (π) ² (π) ²	7.0	7.63
lin12'	$C_{\infty v}$	³ Σ^-	core(σ) ² (π) ² (π) ² (π) ² (π) ² (π) ² (π) ² (π) ² (π) ² (σ) ² (π) ² (π) ¹ (π) ¹	0.0	8.01
cyc12	C_{2v}	¹ A_1	core(a_1) ² (a_1) ² (b_2) ² (a_1) ² (b_1) ² (b_1) ² (a_1) ² (b_2) ² (b_1) ² (a_1) ² (a_2) ² (b_2) ² (b_1) ² (a_1) ² (a_2) ² (b_2) ² (b_1) ²	48.3	1.07
cyc12'	C_{2v}	³ B_1	core(a_1) ² (a_1) ² (b_2) ² (a_1) ² (b_1) ² (a_1) ² (a_1) ² (b_2) ² (b_1) ² (a_1) ² (a_2) ² (b_2) ² (b_1) ² (a_1) ² (a_2) ² (b_2) ² (b_1) ² (a_1) ¹	64.7	0.69
C ₁₃ S				-893.275 516	
lin13	$C_{\infty v}$	¹ Σ^+	core(σ) ² (π) ² (π) ² (π) ² (π) ² (π) ² (π) ² (π) ² (π) ² (σ) ² (π) ² (π) ²	0.0	8.93
lin13'	$C_{\infty v}$	³ Σ^-	core(σ) ² (π) ² (π) ² (π) ² (π) ² (π) ² (π) ² (π) ² (π) ² (σ) ² (π) ² (π) ¹ (π) ¹	21.2	5.49
cyc13	C_{2v}	¹ A_1	core(a_1) ² (a_1) ² (b_2) ² (a_1) ² (b_1) ² (b_1) ² (a_1) ² (b_1) ² (a_1) ² (b_2) ² (a_2) ² (b_2) ² (b_1) ² (a_1) ² (a_2) ² (b_2) ² (b_1) ²	39.7	0.05
cyc13'	C_{2v}	³ A_2	core(a_1) ² (a_1) ² (b_2) ² (b_1) ² (a_1) ² (b_1) ² (a_1) ² (b_1) ² (a_1) ² (b_2) ² (a_2) ² (b_2) ² (b_1) ² (a_1) ² (a_2) ² (b_2) ² (b_1) ²	38.2	1.48

^a Total energies in hartree.lin_n: linear C_nS isomer, cycn: cyclic C_nS isomer; ': triplet.

Table 1(b)

Optimized geometries (distances in angstroms, angles in degrees) for the C_nS species ($6 \leq n \leq 13$) obtained with a DFT/B3LYP/6-311G* method. The geometries are displayed in Fig. 1

Isomers	Structural parameters
C_6S	
lin6	$d1 = 1.567 d2 = 1.276 d3 = 1.282 d4 = 1.272 d5 = 1.293 d6 = 1.292$
lin6'	$d1 = 1.566 d2 = 1.275 d3 = 1.281 d4 = 1.272 d5 = 1.291 d6 = 1.294$
cyc6	$d1 = 1.758 d2 = 1.235 d3 = 1.361 d4 = 1.241 \theta = 94.5 \theta_2 = 137.2 \theta_3 = 141.4 \theta_4 = 124.2$
cyc6'	$d1 = 1.723 d2 = 1.260 d3 = 1.341 d4 = 1.369 \theta_1 = 101.9 \theta_2 = 125.8 \theta_3 = 157.6 \theta_4 = 115.7$
C_7S	
lin7	$d1 = 1.558 d2 = 1.278 d3 = 1.270 d4 = 1.281 d5 = 1.266 d6 = 1.293 d7 = 1.282$
lin7'	$d1 = 1.576 d2 = 1.275 d3 = 1.287 d4 = 1.276 d5 = 1.282 d6 = 1.289 d7 = 1.302$
cyc7	$d1 = 1.706 d2 = 1.249 d3 = 1.319 d4 = 1.289 \theta_1 = 91.4 \theta_2 = 151.5 \theta_3 = 141.7 \theta_4 = 141.3 \theta_5 = 119.7$
cyc7'	$d1 = 1.725 d2 = 1.256 d3 = 1.311 d4 = 1.339 \theta_1 = 94.9 \theta_2 = 140.0 \theta_3 = 150.1 \theta_4 = 158.3 \theta_5 = 88.3$
C_8S	
lin8	$d1 = 1.566 d2 = 1.276 d3 = 1.280 d4 = 1.274 d5 = 1.282 d6 = 1.270 d7 = 1.293 d8 = 1.289$
lin8'	$d1 = 1.566 d2 = 1.275 d3 = 1.279 d4 = 1.273 d5 = 1.281 d6 = 1.270 d7 = 1.292 d8 = 1.291$
cyc8	$d1 = 1.679 d2 = 1.371 d3 = 1.414 d4 = 1.254 d5 = 1.343 \theta_1 = 83.5 \theta_2 = 123.2 \theta_3 = 138.5 \theta_4 = 118.7 \theta_5 = 124.9$
cyc8'	$d1 = 1.717 d2 = 1.416 d3 = 1.412 d4 = 1.360 d5 = 1.256 \theta_1 = 94.2 \theta_2 = 110.9 \theta_3 = 128.2 \theta_4 = 113.9 \theta_5 = 126.3$
C_9S	
lin9	$d1 = 1.560 d2 = 1.277 d3 = 1.272 d4 = 1.279 d5 = 1.269 d6 = 1.283 d7 = 1.265 d8 = 1.294 \theta_9 = 1.282$
lin9'	$d1 = 1.572 d2 = 1.274 d3 = 1.284 d4 = 1.274 d5 = 1.281 d6 = 1.278 d7 = 1.276 d8 = 1.290 \theta_9 = 1.296$
cyc9	$d1 = 1.685 d2 = 1.314 d3 = 1.258 d4 = 1.343 d5 = 1.433 \theta_1 = 106.5 \theta_2 = 135.9 \theta_3 = 161.8 \theta_4 = 159.5 \theta_5 = 180.0 \theta_6 = 58.9$
cyc9'	$d1 = 1.708 d2 = 1.278 d3 = 1.283 d4 = 1.316 d5 = 1.391 \theta_1 = 95.3 \theta_2 = 142.9 \theta_3 = 162.8 \theta_4 = 160.0 \theta_5 = 173.7 \theta_6 = 65.9$
$C_{10}S$	
lin10	$d1 = 1.566 d2 = 1.275 d3 = 1.279 d4 = 1.274 d5 = 1.279 d6 = 1.272 d7 = 1.282 d8 = 1.269 d9 = 1.293 d10 = 1.289$
lin10'	$d1 = 1.566 d2 = 1.276 d3 = 1.279 d4 = 1.275 d5 = 1.280 d6 = 1.273 d7 = 1.283 d8 = 1.269 d9 = 1.294 d10 = 1.287$
cyc10	$d0 = 1.375 d1 = 1.825 d2 = 1.327 d3 = 1.263 d4 = 1.301 d5 = 1.270 d6 = 1.301 \theta = 44.3 \theta_1 = 204.5 \theta_2 = 145.5 \theta_3 = 155.4 \theta_4 = 141.4 \theta_5 = 141.0$
cyc10'	$d0 = 1.358 d1 = 1.829 d2 = 1.334 d3 = 1.275 d4 = 1.294 d5 = 1.352 d6 = 1.241 \theta = 43.6 \theta_1 = 205.1 \theta_2 = 144.3 \theta_3 = 163.5 \theta_4 = 125.6 \theta_5 = 149.6$
$C_{11}S$	
lin11	$d1 = 1.561 d2 = 1.277 d3 = 1.273 d4 = 1.279 d5 = 1.271 d6 = 1.281 d7 = 1.269 d8 = 1.283 d9 = 1.265 d10 = 1.295 d11 = 1.282$
lin11'	$d1 = 1.570 d2 = 1.274 d3 = 1.282 d4 = 1.274 d5 = 1.281 d6 = 1.275 d7 = 1.279 d8 = 1.279 d9 = 1.274 d10 = 1.292 d11 = 1.293$
cyc11	$d0 = 1.348 d1 = 1.834 d2 = 1.347 d3 = 1.258 d4 = 1.322 d5 = 1.282 d6 = 1.308 \theta = 43.1 \theta_1 = 209.5 \theta_2 = 140.2 \theta_3 = 173.8 \theta_4 = 125.2 \theta_5 = 171.7 \theta_6 = 115.9$
cyc11'	$d0 = 1.430 d1 = 1.792 d2 = 1.311 d3 = 1.281 d4 = 1.293 d5 = 1.286 d6 = 1.294 \theta = 47.0 \theta_1 = 204.8 \theta_2 = 145.1 \theta_3 = 164.5 \theta_4 = 137.4 \theta_5 = 158.1 \theta_6 = 128.9$
$C_{12}S$	
lin12	$d1 = 1.566 d2 = 1.275 d3 = 1.278 d4 = 1.275 d5 = 1.279 d6 = 1.274 d7 = 1.280 d8 = 1.272 d9 = 1.283 d10 = 1.268 d11 = 1.295 d12 = 1.286$
lin12'	$d1 = 1.566 d2 = 1.275 d3 = 1.278 d4 = 1.275 d5 = 1.278 d6 = 1.274 d7 = 1.280 d8 = 1.272 d9 = 1.282 d10 = 1.268 d11 = 1.293 d12 = 1.288$
cyc12	$d0 = 1.428 d1 = 1.785 d2 = 1.309 d3 = 1.279 d4 = 1.288 d5 = 1.285 d6 = 1.284 d7 = 1.288 \theta = 47.2 d1 = 196.6 \theta_2 = 152.0 \theta_3 = 162.5 \theta_4 = 147.3 \theta_5 = 152.0 \theta_6 = 145.9$
cyc12'	$d0 = 1.413 d1 = 1.790 d2 = 1.313 d3 = 1.276 d4 = 1.289 d5 = 1.287 d6 = 1.283 d7 = 1.291 \theta = 46.5 \theta_1 = 204.4 \theta_2 = 158.3 \theta_3 = 155.5 \theta_4 = 153.7 \theta_5 = 147.2 \theta_6 = 147.6$
$C_{13}S$	
lin13	$d1 = 1.562 d2 = 1.276 d3 = 1.274 d4 = 1.278 d5 = 1.272 d6 = 1.280 d7 = 1.270 d8 = 1.282 d9 = 1.268 d10 = 1.284 d11 = 1.265 d12 = 1.295 d13 = 1.282$
lin13'	$d1 = 1.569 d2 = 1.270 d3 = 1.290 d4 = 1.264 d5 = 1.294 d6 = 1.262 d7 = 1.294 d8 = 1.265 d9 = 1.288 d10 = 1.272 d11 = 1.277 d12 = 1.289 d13 = 1.292$
cyc13	$d0 = 1.349 d1 = 1.832 d2 = 1.336 d3 = 1.254 d4 = 1.305 d5 = 1.269 d6 = 1.295 d7 = 1.284 \theta = 43.2 \theta_1 = 206.6 \theta_2 = 163.8 \theta_3 = 152.6 \theta_4 = 164.1 \theta_5 = 140.4 \theta_6 = 163.7 \theta_7 = 134.4$
cyc13'	$d0 = 1.393 d1 = 1.799 d2 = 1.323 d3 = 1.265 d4 = 1.299 d5 = 1.273 d6 = 1.292 d7 = 1.283 \theta = 45.5 \theta_1 = 209.4 \theta_2 = 153.2 \theta_3 = 165.2 \theta_4 = 150.9 \theta_5 = 156.5 \theta_6 = 145.7 \theta_7 = 152.8$

Table 2(a)

Valence orbital configurations, total energies (in hartree), relative stabilities ΔE (in kcal mol⁻¹) and dipole moments (in debye) of the different C_nS ($13 \leq n \leq 20$) structures obtained with a DFT/B3LYP/6-31G* method. The symmetry (point group) and the electronic state of the different structures are also given

Isomer	Point group	State	Electronic configuration	ΔE^a	μ
$C_{13}S$	$C_{\infty v}$	$^1\Sigma^+$	$\text{core}(\sigma)^2(\sigma)^2(\sigma)^2(\sigma)^2(\sigma)^2(\sigma)^2(\sigma)^2(\sigma)^2(\sigma)^2(\sigma)^2(\sigma)^2(\sigma)^2(\sigma)^2(\pi)^2$ $(\pi)^2(\pi)^2(\pi)^2(\pi)^2(\pi)^2(\pi)^2(\pi)^2(\pi)^2(\pi)^2(\pi)^2(\pi)^2(\pi)^2(\pi)^2(\pi)^2$	-893.129782	7.67
		3A_2	$\text{core}(a_1)^2(a_1)^2(b_2)^2(a_1)^2(b_2)^2(a_1)^2(b_2)^2(a_1)^2(b_2)^2(a_1)^2(b_2)^2(a_1)^2(b_2)^2(a_1)^2$ $(b_1)^2(a_1)^2(b_1)^2(a_1)^2(b_2)^2(a_2)^2(b_2)^2(b_1)^2(a_1)^2(a_2)^2(b_2)^2(b_1)^2(a_1)^2(a_2)^2$ $(b_1)^1(b_2)^1$	37.2	0.81
$C_{14}S$	$C_{\infty v}$	$^3\Sigma^-$	$\text{core}(\sigma)^2(\sigma)^2(\sigma)^2(\sigma)^2(\sigma)^2(\sigma)^2(\sigma)^2(\sigma)^2(\sigma)^2(\sigma)^2(\sigma)^2(\sigma)^2(\sigma)^2(\pi)^2$ $(\pi)^2(\pi)^2(\pi)^2(\pi)^2(\pi)^2(\pi)^2(\pi)^2(\pi)^2(\pi)^2(\pi)^2(\pi)^2(\pi)^2(\pi)^2(\pi)^2$	-931.199	184
		1A_1	$\text{core}(a_1)^2(a_1)^2(b_2)^2(a_1)^2(b_2)^2(a_1)^2(b_2)^2(a_1)^2(b_2)^2(a_1)^2(b_2)^2(a_1)^2$ $(a_1)^2(b_1)^2(a_1)^2(b_1)^2(a_1)^2(b_2)^2(a_2)^2(b_2)^2(b_1)^2(a_1)^2(a_2)^2(b_2)^2(b_1)^2(a_1)^2$ $(a_2)^2(b_2)^2(b_1)^2$	0.0	7.82
$C_{15}S$	$C_{\infty v}$	$^1\Sigma^+$	$\text{core}(\sigma)^2(\sigma)^2(\sigma)^2(\sigma)^2(\sigma)^2(\sigma)^2(\sigma)^2(\sigma)^2(\sigma)^2(\sigma)^2(\sigma)^2(\sigma)^2(\sigma)^2(\pi)^2$ $(\pi)^2(\pi)^2(\pi)^2(\pi)^2(\pi)^2(\pi)^2(\pi)^2(\pi)^2(\pi)^2(\sigma)^2(\pi)^2(\pi)^2(\pi)^2(\pi)^2(\pi)^1(\pi)^1$	-969.287	904
		1A_1	$\text{core}(a_1)^2(a_1)^2(b_2)^2(a_1)^2(b_2)^2(a_1)^2(b_2)^2(a_1)^2(b_2)^2(a_1)^2(b_2)^2(a_1)^2$ $(a_1)^2(b_2)^2(b_1)^2(a_1)^2(b_1)^2(a_1)^2(b_2)^2(a_2)^2(b_2)^2(b_1)^2(a_1)^2(a_2)^2(b_2)^2(b_1)^2$ $(a_1)^2(a_2)^2(b_2)^2(b_1)^2(a_1)^2$	0.0	8.57
$C_{16}S$	$C_{\infty v}$	$^3\Sigma^-$	$\text{core}(\sigma)^2(\sigma)^2(\sigma)^2(\sigma)^2(\sigma)^2(\sigma)^2(\sigma)^2(\sigma)^2(\sigma)^2(\sigma)^2(\sigma)^2(\sigma)^2(\sigma)^2(\pi)^2$ $(\sigma)^2(\pi)^2(\pi)^2(\pi)^2(\pi)^2(\pi)^2(\pi)^2(\pi)^2(\pi)^2(\pi)^2(\pi)^2(\pi)^2(\pi)^2(\sigma)^2$ $(\pi)^2(\pi)^2(\pi)^1(\pi)^1$	-1007.358	905
		1A_1	$\text{core}(a_1)^2(a_1)^2(b_2)^2(a_1)^2(b_2)^2(b_1)^2(b_2)^2(a_1)^2(b_2)^2(a_1)^2(b_2)^2(a_1)^2$ $(b_2)^2(a_1)^2(b_1)^2(a_1)^2(b_1)^2(b_1)^2(b_2)^2(a_2)^2(b_2)^2(b_1)^2(a_1)^2(a_2)^2(b_2)^2$ $(b_1)^2(a_1)^2(a_2)^2(b_2)^2(b_1)^2(a_1)^2(b_1)^2$	18.8	0.93
$C_{17}S$	$C_{\infty v}$	$^1\Sigma^+$	$\text{core}(\sigma)^2(\sigma)^2(\sigma)^2(\sigma)^2(\sigma)^2(\sigma)^2(\sigma)^2(\sigma)^2(\sigma)^2(\sigma)^2(\sigma)^2(\sigma)^2(\sigma)^2(\pi)^2$ $(\sigma)^2(\sigma)^2(\pi)^2(\pi)^2(\pi)^2(\pi)^2(\pi)^2(\pi)^2(\pi)^2(\pi)^2(\pi)^2(\pi)^2(\pi)^2(\pi)^2$ $(\sigma)^2(\pi)^2(\pi)^2(\pi)^2$	-1045.446	206
		1A_1	$\text{core}(a_1)^2(a_1)^2(b_2)^2(a_1)^2(b_2)^2(a_1)^2(b_2)^2(a_1)^2(b_2)^2(a_1)^2(b_2)^2(a_1)^2$ $(b_2)^2(a_1)^2(b_2)^2(a_1)^2(b_1)^2(a_1)^2(b_2)^2(a_1)^2(b_2)^2(a_2)^2(b_2)^2(b_1)^2(a_1)^2(a_2)^2$ $(b_2)^2(b_1)^2(a_1)^2(a_2)^2(b_2)^2(b_1)^2(a_1)^2(a_2)^2(b_1)^2$	0.0	9.47
$C_{18}S$	$C_{\infty v}$	$^3\Sigma^-$	$\text{core}(\sigma)^2(\sigma)^2(\sigma)^2(\sigma)^2(\sigma)^2(\sigma)^2(\sigma)^2(\sigma)^2(\sigma)^2(\sigma)^2(\sigma)^2(\sigma)^2(\sigma)^2(\pi)^2$ $(\sigma)^2(\sigma)^2(\sigma)^2(\pi)^2(\pi)^2(\pi)^2(\pi)^2(\pi)^2(\pi)^2(\pi)^2(\pi)^2(\pi)^2(\pi)^2(\pi)^2(\pi)^2$ $(\pi)^2(\pi)^2(\pi)^2(\sigma)^2(\pi)^2(\pi)^2(\pi)^1(\pi)^1$	-1083.527	409
		1A_1	$\text{core}(a_1)^2(a_1)^2(b_2)^2(a_1)^2(b_2)^2(a_1)^2(b_2)^2(a_1)^2(b_2)^2(a_1)^2(b_2)^2(a_1)^2$ $(b_2)^2(a_1)^2(b_2)^2(a_1)^2(a_1)^2(b_1)^2(a_1)^2(b_1)^2(b_1)^2(a_1)^2(b_2)^2(a_2)^2(b_2)^2(a_1)^2$ $(b_2)^2(b_1)^2(a_1)^2(a_2)^2(b_2)^2(b_1)^2(a_1)^2(a_2)^2(b_1)^2$	5.6	9.49
$C_{19}S$	$C_{\infty v}$	$^1\Sigma^+$	$\text{core}(\sigma)^2(\sigma)^2(\sigma)^2(\sigma)^2(\sigma)^2(\sigma)^2(\sigma)^2(\sigma)^2(\sigma)^2(\sigma)^2(\sigma)^2(\sigma)^2(\sigma)^2(\pi)^2$ $(\sigma)^2(\sigma)^2(\sigma)^2(\sigma)^2(\pi)^2(\pi)^2(\pi)^2(\pi)^2(\pi)^2(\pi)^2(\pi)^2(\pi)^2(\pi)^2(\pi)^2(\pi)^2$ $(\pi)^2(\pi)^2(\pi)^2(\sigma)^2(\pi)^2(\pi)^2(\pi)^2$	-1121.604	638
		1A_1	$\text{core}(a_1)^2(a_1)^2(b_2)^2(a_1)^2(b_2)^2(b_1)^2(b_2)^2(a_1)^2(b_2)^2(a_1)^2(b_2)^2(a_1)^2$ $(b_2)^2(a_1)^2(b_2)^2(a_1)^2(a_1)^2(b_1)^2(a_1)^2(b_1)^2(b_1)^2(a_1)^2(b_2)^2(b_2)^2(b_1)^2$ $(a_1)^2(b_2)^2(b_1)^2(a_1)^2(a_2)^2(b_2)^2(b_1)^2(a_1)^2(a_2)^2(b_2)^2(b_1)^2$	5.7	0.82
$C_{20}S$	$C_{\infty v}$	$^3\Sigma^-$	$\text{core}(\sigma)^2(\sigma)^2(\sigma)^2(\sigma)^2(\sigma)^2(\sigma)^2(\sigma)^2(\sigma)^2(\sigma)^2(\sigma)^2(\sigma)^2(\sigma)^2(\sigma)^2(\pi)^2$ $(\sigma)^2(\sigma)^2(\sigma)^2(\sigma)^2(\pi)^2(\pi)^2(\pi)^2(\pi)^2(\pi)^2(\pi)^2(\pi)^2(\pi)^2(\pi)^2(\pi)^2(\pi)^2$ $(\pi)^2(\pi)^2(\pi)^2(\sigma)^2(\pi)^2(\pi)^2(\sigma)^2(\pi)^2(\pi)^1(\pi)^1$	-1159.677	969
		3B_2	$\text{core}(a_1)^2(a_1)^2(b_2)^2(a_1)^2(b_2)^2(a_1)^2(b_2)^2(a_1)^2(b_2)^2(a_1)^2(b_2)^2(a_1)^2$ $(b_2)^2(a_1)^2(b_2)^2(a_1)^2(b_2)^2(a_1)^2(b_1)^2(a_1)^2(b_1)^2(b_1)^2(a_1)^2(b_2)^2(a_2)^2(b_2)^2$ $(b_1)^2(a_1)^2(a_2)^2(b_2)^2(b_1)^2(a_1)^2(a_2)^2(b_2)^2(b_1)^2(a_1)^2(a_2)^2(b_2)^2(b_1)^2$ $(b_1)^1(a_2)^1$	8.3	0.68

^a Total energies in hartrees.

Table 2(b)

Optimized geometries (distances in angstroms, angles in degrees) for the C_nS species ($13 \leq n \leq 20$) obtained with a DFT/B3LYP/6-31G* method. The geometries are displayed in Fig. 1

Isomers	Structural parameters
$C_{13}S$	
lin13	d1 = 1.567 d2 = 1.280 d3 = 1.281 d4 = 1.282 d5 = 1.278 d6 = 1.284 d7 = 1.276 d8 = 1.286 d9 = 1.274 d10 = 1.288 d11 = 1.271 d12 = 1.299 d13 = 1.288
cyc13'	d0 = 1.393 d1 = 1.805 d2 = 1.330 d3 = 1.270 d4 = 1.306 d5 = 1.278 d6 = 1.299 d7 = 1.289 θ = 43.5 ϕ_1 = 210.2 θ_2 = 150.9 θ_3 = 168.3 θ_4 = 147.7 θ_5 = 160.6 θ_6 = 141.4 θ_7 = 156.9
$C_{14}S$	
lin14'	d1 = 1.571 d2 = 1.279 d3 = 1.284 d4 = 1.279 d5 = 1.283 d6 = 1.279 d7 = 1.284 d8 = 1.278 d9 = 1.285 d10 = 1.276 d11 = 1.288 d12 = 1.273 d13 = 1.298 d14 = 1.293
cyc14	d0 = 1.368 d1 = 1.833 d2 = 1.332 d3 = 1.261 d4 = 1.308 d5 = 1.267 d6 = 1.305 d7 = 1.271 d8 = 1.304 θ = 43.8 ϕ_1 = 209.5 θ_2 = 156.1 θ_3 = 168.7 θ_4 = 152.8 θ_5 = 160.4 θ_6 = 148.9 θ_7 = 151.7
$C_{15}S$	
lin15	d1 = 1.568 d2 = 1.280 d3 = 1.281 d4 = 1.282 d5 = 1.279 d6 = 1.283 d7 = 1.277 d8 = 1.285 d9 = 1.276 d10 = 1.286 d11 = 1.274 d12 = 1.289 d13 = 1.271 d14 = 1.300 d15 = 1.288
cyc15	d0 = 1.352 d1 = 1.840 d2 = 1.343 d3 = 1.255 d4 = 1.318 d5 = 1.269 d6 = 1.312 d7 = 1.284 d8 = 1.302 θ = 43.1 ϕ_1 = 212.0 θ_2 = 154.0 θ_3 = 175.9 θ_4 = 146.0 θ_5 = 175.1 θ_6 = 135.5 θ_7 = 174.8 θ_8 = 129.9
$C_{16}S$	
lin16'	d1 = 1.571 d2 = 1.278 d3 = 1.284 d4 = 1.279 d5 = 1.283 d6 = 1.279 d7 = 1.284 d8 = 1.279 d9 = 1.284 d10 = 1.278 d11 = 1.286 d12 = 1.276 d13 = 1.288 d14 = 1.273 d15 = 1.298 d16 = 1.292
cyc16	d0 = 1.314 d1 = 1.862 d2 = 1.373 d3 = 1.232 d4 = 1.352 d5 = 1.234 d6 = 1.353 d7 = 1.234 d8 = 1.357 d9 = 1.234 θ = 41.3 ϕ_1 = 210.7 θ_2 = 166.6 θ_3 = 162.0 θ_4 = 165.0 θ_5 = 155.9 θ_6 = 161.0 θ_7 = 152.9 θ_8 = 155.3
$C_{17}S$	
lin17	d1 = 1.569 d2 = 1.279 d3 = 1.282 d4 = 1.281 d5 = 1.279 d6 = 1.283 d7 = 1.278 d8 = 1.284 d9 = 1.277 d10 = 1.286 d11 = 1.275 d12 = 1.287 d13 = 1.274 d14 = 1.289 d15 = 1.271 d16 = 1.300 d17 = 1.288
cyc17	d0 = 1.352 d1 = 1.838 d2 = 1.336 d3 = 1.256 d4 = 1.311 d5 = 1.266 d6 = 1.302 d7 = 1.276 d8 = 1.294 d9 = 1.286 θ = 43.1 ϕ_1 = 210.5 θ_2 = 169.5 θ_3 = 160.1 θ_4 = 169.1 θ_5 = 153.5 θ_6 = 168.5 θ_7 = 147.1 θ_8 = 167.9 θ_9 = 144.4
$C_{18}S$	
lin18'	d1 = 1.571 d2 = 1.278 d3 = 1.284 d4 = 1.279 d5 = 1.283 d6 = 1.280 d7 = 1.283 d8 = 1.279 d9 = 1.284 d10 = 1.279 d11 = 1.285 d12 = 1.278 d13 = 1.286 d14 = 1.276 d15 = 1.288 d16 = 1.273 d17 = 1.299 d18 = 1.292
cyc18	d0 = 1.357 d1 = 1.839 d2 = 1.334 d3 = 1.254 d4 = 1.313 d5 = 1.259 d6 = 1.312 d7 = 1.260 d8 = 1.314 d9 = 1.260 d_{10} = 1.315 θ = 43.3 ϕ_1 = 211.0 θ_2 = 166.6 θ_3 = 166.4 θ_4 = 167.8 θ_5 = 159.5 θ_6 = 161.3 θ_7 = 155.4 θ_8 = 160.8 θ_9 = 155.7
$C_{19}S$	
lin19	d1 = 1.569 d2 = 1.279 d3 = 1.282 d4 = 1.281 d5 = 1.280 d6 = 1.283 d7 = 1.279 d8 = 1.284 d9 = 1.278 d10 = 1.285 d11 = 1.276 d12 = 1.286 d13 = 1.275 d14 = 1.288 d15 = 1.273 d16 = 1.290 d17 = 1.270 d18 = 1.300 d19 = 1.288
cyc19	d0 = 1.351 d1 = 1.844 d2 = 1.339 d3 = 1.253 d4 = 1.316 d5 = 1.262 d6 = 1.310 d7 = 1.271 d8 = 1.304 d9 = 1.282 d_{10} = 1.295 θ = 43.0 ϕ_1 = 213.2 θ_2 = 162.6 θ_3 = 175.5 θ_4 = 156.7 θ_5 = 175.3 θ_6 = 150.5 θ_7 = 175.02 θ_8 = 143.8 θ_9 = 175.3
$C_{20}S$	
lin20'	d1 = 1.571 d2 = 1.278 d3 = 1.284 d4 = 1.279 d5 = 1.283 d6 = 1.280 d7 = 1.283 d8 = 1.280 d9 = 1.283 d10 = 1.279 d11 = 1.284 d12 = 1.279 d13 = 1.285 d14 = 1.278 d15 = 1.286 d16 = 1.276 d17 = 1.289 d18 = 1.272 d19 = 1.299 d_{20} = 1.291
cyc20'	d0 = 1.386 d1 = 1.813 d2 = 1.330 d3 = 1.257 d4 = 1.318 d5 = 1.255 d6 = 1.321 d7 = 1.386 d8 = 1.813 d9 = 1.330 d_{10} = 1.257 d11 = 1.318 θ = 44.9 ϕ_1 = 212.7 θ_2 = 166.3 θ_3 = 171.8 θ_4 = 162.7 θ_5 = 169.3 θ_6 = 159.7 θ_7 = 166.4 θ_8 = 156.7 θ_9 = 164.5 θ_{10} = 158.4

SC to a value of the order of 1.57 Å for large n , while for the species with even n , this length is always of the order of 1.57 Å. Such values are of the order of the prototypical double bond length of 1.55 Å existing in carbon disulfide [27]. The CC bond length of the CC

moiety adjacent to S varies more or less uniformly from 1.32 Å for C_2S to a value close to 1.28 Å for large n . The other CC bonds have nearly identical lengths ~1.28–1.30 Å [Fig. 1, Tables 1(b) and 2(b)]. These distances are typical of double bonds (1.35 Å in

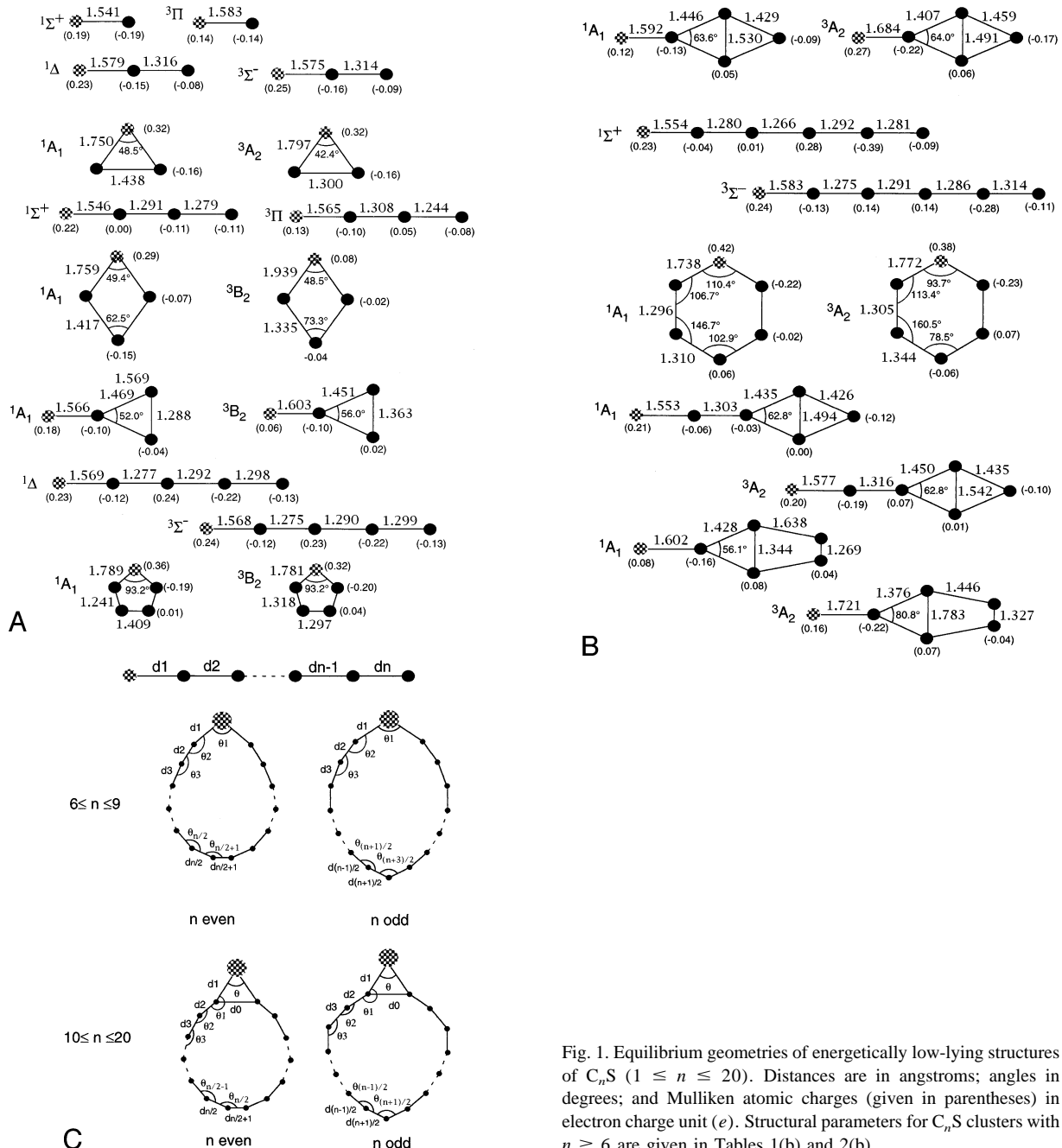


Fig. 1. Equilibrium geometries of energetically low-lying structures of C_nS ($1 \leq n \leq 20$). Distances are in angstroms; angles in degrees; and Mulliken atomic charges (given in parentheses) in electron charge unit (e). Structural parameters for C_nS clusters with $n \geq 6$ are given in Tables 1(b) and 2(b).

ethylene) underlying a clear π bonding in the corresponding structures. No appreciable variation of the CC lengths along the carbon chains also suggests mostly cumulenic structures, i.e. $\ddot{S}—C=C\dots=C=C$ with two lone pairs on the sulphur atom and

one lone pair on the terminal carbon at the other extremity. In these chains the SC bond is weakly polarized with the sulphur atom bearing the positive charge ($<0.25 e$). This is due to the weak difference between the ionization energy values of carbon (11.4

Table 3
Rotational constant (MHz) for the linear C_nS ($1 \leq n \leq 7$) clusters

	DFT/B3LYP/6-311G*	Experiment	Δ^a
CS	24 391.87	24 495.50	+103.13
C_2S	6 425.61	6 477.75 ^b	+52.14
C_3S	2 879.58	2 890.38 ^a	+10.80
C_4S	1 514.09	1 519.16 ^d	+5.07
C_5S	920.88	922.70 ^e	+1.82
C_6S	596.19
C_7S	414.07

^a $\Delta = \text{Experiment-DFT/B3LYP/6-311G}^*$

^b [7].

^c [8].

^d [28].

^e [29].

eV) and sulphur (10.4 eV). Additionally, the charges of the various carbon atoms are all smaller than $\pm 0.3 e$, except the penultimate one which bears a negative charge with a strong absolute value higher than $0.5 e$ when $n > 7$. This result appears in contrast with the one obtained in the case of the linear C_nSi clusters where the SiC bond is always highly polarized and the charge is strongly oscillating along the carbon chain [5,6]. The dipole moment increases very regularly with n , going from 2 D for the diatomic molecule SC to 10 D when $n = 20$ [Tables 1(a) and 2(a)].

Very little experimental information is known for the sulphur carbide clusters as soon as $n \geq 4$. For the linear isomer of C_4S the rotational constant was measured by Hirahara et al. [28] by Fourier transform spectroscopy. These authors find a value of 1.519 165 GHz in good agreement with our theoretical result of 1.514 GHz (Table 3). The rotational constants for the linear isomer of C_5S is experimentally found to be of the order of 0.9227 GHz [29,30] again in very close agreement with the value of 0.921 GHz obtained in the present work. The rotational constants being

strongly dependent on the bond distances, we think that the DFT/B3LYP/6-311G* distances have to be in close agreement with experiment. However, In Table 3, we show that the DFT/B3LYP/6-311G* values of the rotational constants are always smaller than the experimental ones, but that this difference is uniformly reduced when going from $n = 2$ to $n = 5$. This indicates that the SC distances in the linear C_nS series given by this method are systematically overestimated by about 0.003 Å. Unfortunately, no experimental result exists for $n = 6$ or other linear isomers, even though such a determination would be of great interest in this context. A comparison with ab initio calculations at the coupled-cluster single double (triple) [CCSD(T)] level of theory is made in Table 4. The agreement between the two methods CCSD(T) and B3LYP appears very satisfactory, the differences in the corresponding CCSD(T) and B3LYP distances being smaller than 0.01 Å. Considering the well-known fact that the CPU time of DFT methods on the size N of the system is only $O(N^3)$ to $O(N^4)$, whereas very accurate ab initio CCSD(T) scales as $O(N^6)$ to $O(N^7)$, DFT/B3LYP method appears well adapted to medium-sized impurity-containing carbon clusters as already noticed [5,6,19,20].

The next electronic state in the energy ordering for the linear isomers alternates in a regular manner between $^3\Sigma^-$ state for odd $n \geq 5$ and $^1\Delta$ for even n . As reference to Tables 1(a) and 2(a) shows, the $^3\Pi-^1\Sigma^+$ ($n = 1, 3$) or $^3\Sigma^- - ^1\Sigma^+$ ($n \geq 5$) energetic separation between the two lowest linear states for the n -odd clusters is always higher than the $^1\Delta-^3\Sigma^-$ energetic separation corresponding to the $(n + 1)$ -even and $(n - 1)$ -even congeners. This result is not surprising given that the $^1\Sigma^+$ state is associated to fully occupied doubly degenerate π orbitals, which represents a particularly stable situation, while in the

Table 4
Equilibrium bond lengths (in angstroms) for the linear C_5S cluster (the carbon atoms are numbered from the sulphur atom).

method	S-C ₁	C ₁ -C ₂	C ₂ -C ₃	C ₃ -C ₄	C ₄ -C ₅
DFT/B3LYP/6-311G*	1.5539	1.2799	1.2660	1.2915	1.2810
CCSD(T) ^a	1.5459	1.2800	1.2707	1.2924	1.2786

^a [30].

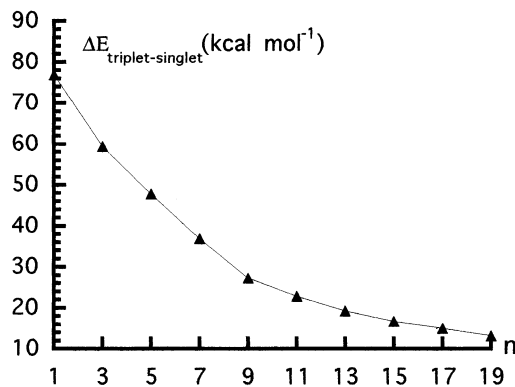


Fig. 2. Computed triplet-singlet energy differences (in kcal mol^{-1}) for the n -odd linear C_nS clusters as a function of n (${}^3\Pi-{}^1\Sigma^+$ for $n = 1, 3$ and ${}^3\Sigma^--{}^1\Sigma^+$ for $n \geq 5$).

${}^3\Sigma^-$ state the doubly degenerate π orbitals are half-filled. Figs. 2 and 3, however, indicate that these energetic separations (${}^3\Pi-{}^1\Sigma^-$ or ${}^3\Sigma^--{}^1\Sigma^+$ for odd n , ${}^1\Delta-{}^3\Sigma^-$ for even n) both alike decrease gradually when going from $n = 1$ to 20. Another noticeable point is that for even n the ${}^1\Delta$ states generally have real frequencies and correspond to local minima on the energy surface while, for odd n , the second linear in the order of energy (${}^3\Pi$ or ${}^3\Sigma^-$) very often possesses imaginary frequencies indicative of saddle points on the energy surface. The SC and CC distances in excited geometries are however mostly similar to the corresponding ones in the respective ground states (${}^1\Sigma^+$ for odd n , ${}^3\Sigma^-$ for even n) except

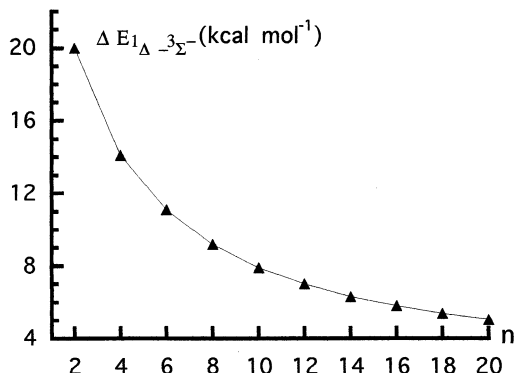


Fig. 3. Energy separation (in kcal mol^{-1}) between the ${}^1\Delta$ and ${}^3\Sigma^-$ states for the n -even C_nS clusters as a function of n .

for the diatomic molecule SC where the SC distance is larger by 0.04 Å than the one relative to the ground state (${}^1\Sigma^+$).

As for the singlet and triplet cyclic forms (labeled cyc in Tables 1–6 and Fig. 4) these are generally located very high in energy, sometimes with relative energies higher than 100 kcal mol⁻¹ above the linear ground state when n is smaller than 9. The lowest cyclic state is indifferently triplet or singlet for $n \leq 8$ and definitely singlet when $n > 8$ (1A_1) except for $n = 13$ (3A_2) and $n = 20$ (3B_2). These cyclic structures very often have one or two imaginary frequencies indicative of saddle points on the energy surface. Structures possessing a bicyclic C_4 entity can even compete with the corresponding monocyclic rings, for instance in the case of C_5S where the SC-capped bicyclic C_4 is located just above the monocyclic C_5S , at only about 4 kcal mol⁻¹. Another typical example is C_4S for which the SC-capped bicyclic C_4 is energetically favored over the monocyclic ring (3B_2) by 6 kcal mol⁻¹. The SC distances in C_nS cyclic structures, ~1.68–1.75 Å, can be ascribed to SC single bonds (1.71 Å in thiophene [27]). For $n \geq 10$, the sulphur atom takes an exohedral position with regard to the carbon monocyclic entity with SC bonds lengths ~1.80 Å indicative of weak SC single bonds. This statement clearly indicates the reluctance for sulphur to incorporate into a carbon monocyclic ring. In all the cyclic structures, the CC distances alternate between double bonds and strong double bonds (the latter ones being intermediate between prototypical double and triple bonds). It is worth noting that for C_{14}S , the energy separation between the linear isomer (${}^3\Sigma^-$) and the cyclic one (1A_1) is very small (~4 kcal mol⁻¹). This weak energy difference between the linear and the cyclic structures (Fig. 4) is due to the high stability of the C_{14} substructure present in the cyclic C_{14}S isomer. As a matter of fact the C_{4n+2} rings, associated with a fourfold periodicity (10, 14, 18, 22, ...) are predicted to be particularly stable species [31,32]. When $15 \leq n \leq 17$, the energetic separation between the cyclic and the linear forms in their lowest states takes moderately high values ~15–19 kcal mol⁻¹. Eventually when $n = 18$, as due to the fourfold periodicity,

Table 5

Vibrational frequencies (in cm^{-1}) and zero-point energy (in kcal mol^{-1}) of the different C_nS ($1 \leq n \leq 11$) clusters calculated with a DFT/6-311G* method. Imaginary frequencies indicate a saddle point on the energy surface. The Hessian index is also given

Structure	Vibrational frequencies	Zero-point energy	Hessian index
CS			
lin1 ^a	1301(σ)	1.9	0
lin1'	1125(σ)	1.6	0
C_2S			
lin2	202(π) 341(π) 853(σ) 1742(σ)	4.5	0
lin2'	265(π) ^d 860(σ) 1723(σ)	4.4	0
cyc2	720(a1) 749(b2) 1182(a1)	3.8	0
cyc2'	683i(b2) 721(a1) 1647(a1)		1
C_3S			
lin3	160(π) ^d 481(π) ^d 739(σ) 1567(σ) 2144(σ)	8.2	0
lin3'	180i(π) 190(π) 192(π) 448(π) 716(σ) 1575(σ) 1979(σ)	7.3	1
cyc3	141(b2) 424(b1) 692(a1) 767(b2) 999(a1) 1454(a1)	6.4	1
cyc3'	552i(b1) 488i(b2) 438(a1) 641(a1) 1262(b2) 1654(a1)	5.7	2
S-cycC3	529i(b2) 440(b1) 442(b2) 709(a1) 1407(a1) 1721(a1)	6.7	1
S-cycC3'	157(b2) 407(b1) 571(b2) 678(a1) 1186(a1) 1550(a1)	6.5	1
C_4S			
lin4	115(π) 131(π) 267(π) 303(π) 384(π) 517(π) 610(σ) 1226(σ) 1816(σ) 2133(σ)	10.7	0
lin4'	127(π) ^d 311(π) ^d 408(π) ^d 612(σ) 1223(σ) 1810(σ) 2118(σ)	10.7	0
cyc4	558i(b2) 291(a2) 289(a1) 341(b1) 648(b2) 683(a1) 1143(a1) 1905(a1) 1918(b2)	9.9	2
cyc4'	192i(a2) 307(b1) 563(a1) 580(b2) 690(a1) 983(b2) 1371(a1) 1630(a1) 2925(b2)	12.9	1
S-bicycC4	218(b1) 347(b2) 591(b1) 617(b2) 624(a1) 946(b2) 989(a1) 1390(a1) 1472(a1)	10.3	0
S-bicycC4'	3369i(b2) 70i(b2) 29i(b1) 355(b2) 439(b1) 551(a1) 952(a1) 1227(a1) 1457(a1)	7.1	3
C_5S			
lin5	76(π) ^d 211(π) ^d 411(π) ^d 496(π) ^d 543(σ) 1091(σ) 1656(σ) 2088(σ) 2239(σ)	14.3	0
lin5'	728i(π) 37i(π) 95(π) 121(π) 214(π) 309(π) 343(π) 451(π) 523(σ) 1009(σ) 1501(σ) 1747(σ) 1894(σ)	11.7	2
cyc5	402(b1) 450(a1) 452(b1) 486(a2) 507(a1) 577(b2) 594(b2) 735(a1) 1229(a1) 1357(b2) 1570(b2) 1788(a1)	14.5	0
cyc5'	344(a1) 352(b1) 407(a2) 531(b2) 582(b1) 626(b2) 660(a1) 737(a1) 1020(b2) 1216(a1) 1271(b2) 1788(a1)	13.6	0
SC-bicycC4	131(b1) 147(b2) 349(b1) 417(b2) 519(b1) 543(a1) 634(b2) 802(b2) 986(a1) 1297(a1) 1437(a1) 1943(a1)	13.2	0
SC-bicycC4'	129(b2) 64(b1) 223(b1) 345(b2) 476(b1) 520(a1) 585(b2) 826(b2) 918(a1) 1190(a1) 1349(a1) 1730(a1)	11.2	0
S-bicycC5	691i(b2) 436i(a2) 255i(b2) 184i(b1) 300(b2) 340(b1) 450(a1) 880(a1) 892(b2) 1194(a1) 1636(a1) 1786(a1)	10.7	4
S-bicycC5'	636i(b2) 185(b1) 204(b1) 227(b2) 461(a1) 526(a2) 661(b2) 711(a1) 845(b2) 1081(a1) 1484(a1) 1603(a1)	11.4	1
C_6S			
lin6	68(π) ^d 164(π) 188(π) 290(π) 294(π) 350(π) 432(π) 450(π) 476(σ) 589(σ) 939(σ) 1411(σ) 1848(σ) 2093(σ) 2146(σ)	16.9	0
lin6'	70(π) ^d 176(π) ^d 307(π) ^d 476(π) ^d 476(σ) 938(σ) 1410(σ) 1838(σ) 2091(σ) 2133(σ)	16.6	0
cyc6	313i(a2) 123i(b2) 250i(b1) 255(a2) 312(a1) 391(b1) 392(b2) 532(b2) 541(a1) 688(a1) 1132(a1) 1278(b2) 1958(a1) 2013(a1) 2033(b2)	16.8	3
cyc6'	120(b2) 240(b1) 308(a2) 377(a1) 419(b1) 513(b2) 555(b2) 558(a2) 599(a1) 735(a1) 1123(a1) 1170(b2) 1490(a1) 1746(b2) 1943(a1)	17.0	0
C_7S			
lin7	32(π) ^d 119(π) ^d 233(π) ^d 309(π) ^d 432(σ) 450(π) ^d 615(π) ^d 855(σ) 1285(σ) 1713(σ) 2010(σ) 2212(σ) 2232(σ)	20.4	0
lin7'	41(π) 55(π) 83(π) 112(π) 153(π) 191(π) 269(π) 322(π) 370(π) 392(π) 424(σ) 455(π) 591(π) 822(σ) 1232(σ) 1596(σ) 1642(σ) 1932(σ) 2038(σ)	18.2	0

(continued)

Table 5 (continued)

Structure	Vibrational frequencies	Zero-point energy	Hessian index
cyc7	735 <i>i</i> (b1) 468 <i>i</i> (a2) 223 <i>i</i> (a2) 46 <i>i</i> (b1) 292(b1) 305(a1) 328(b2) 458(a1) 501(a1) 509(b2) 652(b2) 672(a1) 1117(a1) 1270(b2) 1732(a1) 1761(b2) 1930(a1) 2023(b2)	19.4	3
cyc7'	174(b1) 193(a2) 230(b1) 276(b2) 277(b1) 321(a1) 382(a2) 419(a1) 478(b2) 516(a1) 530(b2) 664(a1) 916(b2) 1062(a1) 1373(b2) 1699(a1) 1809(b2) 1946(a1)	19.0	0
C ₈ S			
lin8	180 <i>i</i> (π) 38 <i>i</i> (π) 44(π) 72(π) 126(π) 157(π) 221(π) 234(π) 353(π) 358(π) 390(σ) 457(π) 519(π) 621(π) 723(π) 766(σ) 1146(σ) 1520(σ) 1851(σ) 2062(σ) 2097(σ) 2174(σ)	22.7	2
lin8'	47(π) ^d 111(π) ^d 197(π) ^d 317(π) ^d 353(π) ^d 387(σ) 543(π) ^d 760(σ) 924(σ) 1137(σ) 1508(σ) 1837(σ) 2052(σ) 2118(σ) 2178(σ)	24.2	0
cyc8	59(b1) 213(b1) 297(a2) 327(b2) 331(a2) 406(b2) 438(a1) 455(b1) 475(b2) 513(a1) 633(a2) 713(b2) 743(a1) 916(a1) 1027(a1) 1067(b2) 1292(a1) 1499(a1) 1544(b2) 1810(a1) 1917(b2)	23.8	0
cyc8'	2448 <i>i</i> (b2) 184(b1) 259(a2) 283(b2) 353(b1) 411(b2) 448(a2) 477(a1) 578(a1) 581(b2) 590(b1) 671(a2) 792(a1) 850(b2) 904(a1) 1124(b2) 1187(a1) 1234(a1) 1346(b2) 1358(a1) 1892(a1)	22.2	1
C ₉ S			
lin9	35(π) ^d 84(π) ^d 154(π) ^d 261(π) ^d 337(π) ^d 356(σ) 459(π) ^d 672(π) ^d 703(σ) 1051(σ) 1180(π) ^d 1397(σ) 1728(σ) 1980(σ) 2136(σ) 2202(σ) 2257(σ)	26.8	0
lin9'	273 <i>i</i> (π) 262 <i>i</i> (π) 37(π) 39(π) 100(π) 109(π) 181(π) 193(π) 279(π) 282(π) 338(π) 356(σ) 433(π) 490(π) 557(π) 694(σ) 712(π) 808(π) 1035(σ) 1069(σ) 1568(σ) 1688(σ) 1932(σ) 2079(σ) 2092(σ)	24.8	2
cyc9	2141 <i>i</i> (b2) 68 <i>i</i> (b1) 169(b1) 201(a1) 226(a2) 240(b2) 357(b2) 368(b1) 420(a1) 424(b1) 470(a2) 528(b2) 548(b2) 554(a1) 565(a1) 628(a1) 794(b2) 855(a1) 1034(a1) 1376(a1) 1462(b2) 1586(b2) 1717(a1) 2040(a1)	23.7	2
cyc9'	99(b1) 165(a2) 242(a1) 251(b1) 262(b2) 373(a1) 377(b1) 400(b1) 407(b2) 421(a2) 460(b2) 460(a2) 500(a1) 544(b2) 598(a1) 698(b2) 729(a1) 913(a1) 1215(b2) 1403(a1) 1672(b2) 1798(a1) 2013(a1) 2278(b2)	26.1	0
C ₁₀ S			
lin10'	33(π) ^d 76(π) ^d 131(π) ^d 203(π) ^d 276(π) ^d 327(σ) 367(π) ^d 513(π) ^d 644(σ) 765(π) ^d 959(σ) 1273(σ) 1375(π) ^d 1572(σ) 1845(σ) 2025(σ) 2052(σ) 2168(σ) 2191(σ)	0	
cyc10	144 <i>i</i> (b2) 94(b1) 164(b2) 201(a1) 221(a2) 246(b1) 289(b2) 330(a2) 394(a1) 407(b1) 420(a2) 442(b2) 465(b1) 466(a1) 502(a2) 561(a1) 609(b2) 815(a1) 1009(b2) 1033(a1) 1385(a1) 1471(b2) 1541(a1) 1834(a1) 1938(b2) 2045(a1) 2087(b2)	30.0	1
C ₁₁ S			
lin11	26(π) ^d 72(π) ^d 137(π) ^d 217(π) ^d 307(σ) 310(π) ^d 426(π) ^d 495(π) ^d 571(π) ^d 607(σ) 694(π) ^d 904(σ) 925(π) ^d 1200(σ) 1484(σ) 1755(σ) 1958(σ) 2126(σ) 2144(σ) 2235(σ) 2262(σ)	35.3	0
cyc11	59(a1) 81(b2) 94(b1) 154(a2) 181(b2) 207(b1) 255(a1) 350(b1) 428(b2) 430(a2) 440(a1) 489(b2) 509(b2) 510(a1) 524(b1) 533(a2) 546(b1) 581(a2) 619(a1) 814(a1) 919(b2) 1022(a1) 1320(b2) 1373(a1) 1611(b2) 1777(a1) 1902(b2) 2027(a1) 2095(a1) 2103(b2)	34.2	0

^a linn: linear C_nS isomer, cycn: cyclic C_nS isomer; ': triplet.

the cyclic structure is, in this case, energetically favored over the linear isomer, even though the latter one lies only 5.6 kcal mol⁻¹ higher (Fig. 4). That the linear arrangement remains the most stable structure up to such a high value of *n* appears in contrast with the results obtained for the pure C_{*n*} clusters. In the

latter compounds, the cyclic geometry becomes definitely more stable than the linear one as soon as *n* is larger than 10 (for *n* < 10 the ground state geometry for the pure carbon clusters alternates between cyclic and linear arrangement [20]). A simple explanation is that whereas the carbon atom is tetravalent and can

Table 6
DFT/B3LYP rotational constants (in GHz) for the low-lying C_nS clusters calculated with a 6-311G* basis set for $1 \leq n \leq 13$ and a 6-31G* basis set for $13 \leq n \leq 20$

Structures	A	B	C
lin1 ^a	0.000	24.392	24.392
lin1'	0.000	23.112	23.112
lin2	0.000	6.397	6.397
lin2'	0.000	6.425	6.425
cyc2 ^a	40.716	14.489	10.686
lin3	0.000	2.880	2.880
cyc3	38.945	6.349	5.439
S-cycC3'	45.311	4.380	3.994
lin4	0.000	1.511	1.511
lin4'	0.000	1.514	1.514
S-bicycC4	35.964	2.696	2.508
lin5	0.000	0.921	0.921
cyc5	6.824	4.476	2.703
cyc5'	8.795	3.573	2.541
SC-bicycC4	37.720	1.391	1.342
SC-bicycC4'	35.407	1.369	1.318
lin6	0.000	0.596	0.596
lin6'	0.000	0.596	0.596
cyc6'	5.455	2.621	1.770
lin7	0.000	0.414	0.414
lin7'	0.000	0.409	0.409
cyc7'	4.642	1.731	1.261
cyc8	5.008	1.225	0.984
lin8'	0.000	0.297	0.297
lin9	0.000	0.223	0.223
cyc9'	3.388	0.905	0.714
lin10'	0.000	0.170	0.170
lin11	0.000	0.134	0.134
cyc11	1.635	0.628	0.453
lin12'	0.000	0.107	0.107
lin13 ^b	0.000	0.087	0.087
cyc13' ^b	0.999	0.430	0.300
lin13 ^c	0.000	0.086	0.086
cyc13' ^c	0.995	0.427	0.299
lin14'	0.000	0.071	0.071
cyc14	0.829	0.351	0.246
lin15	0.000	0.059	0.059
cyc15	0.683	0.300	0.208
lin16'	0.000	0.050	0.050
cyc16	0.550	0.252	0.252
lin17	0.000	0.042	0.042
cyc17	0.461	0.223	0.150
lin18'	0.000	0.036	0.036
cyc18	0.400	0.190	0.129
lin19	0.000	0.032	0.032
cyc19	0.343	0.166	0.112
lin20'	0.000	0.027	0.027
cyc20'	0.286	0.148	0.097

^a linn: linear C_nS isomer, cycn: cyclic C_nS isomer; ': triplet.

^b 6-311G*.

^c 6-31G*.

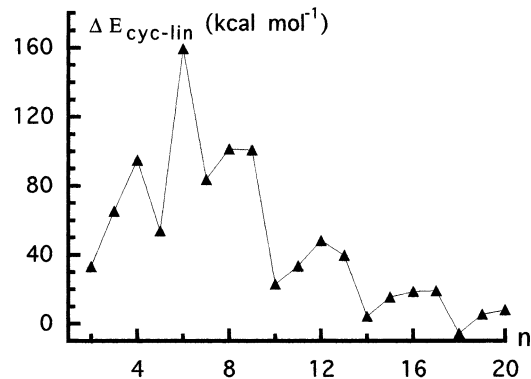


Fig. 4. Energy separation between the lowest energy cyclic and linear structures for the C_nS clusters as a function of n . A negative value indicates that the linear isomer is less stable than the corresponding cyclic one.

make two double bonds producing a very stable cumulenic ring [20,33], the sulphur atom is mainly divalent and can only partake in an unique double bond in a terminal position of a carbon chain. C_nSi clusters become also cyclic when $n \geq 10$ as in the case of pure C_n clusters but the Si atom is bound to the outside of the monocyclic ring. The principal reason is that silicon, even though tetravalent, prefers to form single bonds and that the nature of its double bonds notably differs from that of normal $C=C$ bonds [34]. Thus, as Si replaces C in a pure carbon cluster leads to a distortion of the structure due to the fact that silicon–carbon bond is larger than carbon–carbon bond [34]. It is remarkable that the cyclic isomers of the C_nS clusters look like the corresponding C_nSi ones as soon as $n \geq 10$. In the same way, the sulphur atom (replacing Si) lies outside the carbon monocyclic ring and form two single bonds ($d_{SC} \sim 1.75\text{--}1.80 \text{ \AA}$) with the adjacent carbons (Fig. 1). But the difference is that the cyclic C_nSi are energetically favored for small values of n (for instance C_3Si), while linear C_nS persists as ground state geometry to large size clusters ($n = 17$). This reveals that large S-doped C_n clusters would have properties very different from other impurity-containing C_n clusters such as C_nB , C_nN , or C_nSi [1,2]. For instance incorporating a sulphur atom in a carbon chain may presumably hinder some structural rearrangements like the one

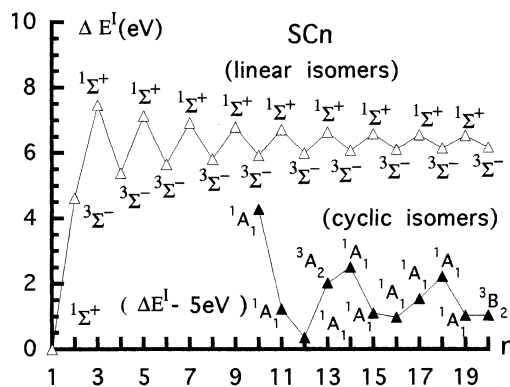


Fig. 5. Incremental binding energies (eV) for the linear and cyclic C_nS clusters vs the number of carbon atoms.

described by Hunter et al. [35] for synthesis of a fullerene fragment from conversion of a linear chain. Formation of a $C_{59}S$ fullerene can thus be precluded or, at least, considerably distorted with regard to pure C_{60} , as early suggested by Kurita [36].

Relative intensity distribution of the doped-carbon clusters synthesized in various experiments is generally deduced from mass spectroscopy measurements [1]. Theoretical prediction for these intensities can be made here for the linear C_nS clusters. The typical alternation for the ground state of these isomers (${}^1\Sigma^+$, ${}^3\Sigma^-$) can be related to the relative stability of these isomers. Introducing the *incremental binding energy* ΔE^I [37] as the change in energy accompanying the following process:



We have

$$\Delta E^I = \Delta E_a(C_nS) - \Delta E_a(C_{n-1}S)$$

where ΔE_a corresponds to the atomization energy [38]. The quantity ΔE^I gauges the relative stabilities of C_nS compounds. From Fig. 5, we show that the linear species containing an odd number of carbon atoms are more stable than the even $n - 1$ and $n + 1$ congeners with a remarkable regularity from $n = 1$ to $n = 20$. This effect is ultimately fastened to the filling of the last doubly degenerate π level. For even n , the latter orbitals are half-filled, while they are fully

occupied for odd n [32]. A similar conclusion has been given for the C_n , C_n^+ , C_nSi , C_nSi^+ clusters [6] and is in agreement with an earlier prediction of Pitzer and Clementi [39] relative to pure C_n clusters.

4. Conclusion

Density functional theory calculations have been carried out for $C_{1-20}S$ clusters. Linear isomeric geometries are found to be the most stable structures when $1 \leq n \leq 17$. The electronic ground state is predicted to be ${}^1\Sigma^+$ or ${}^3\Sigma^-$ alternately depending on whether n is odd or even. For values of n smaller than 14, the lowest-energy cyclic isomer is generally located well above the linear ground state. Additionally, these cyclic structures very often possess one or two imaginary frequencies and thus correspond to saddle points on the energy surface. However, for $n = 18$ the linear arrangement is found to be less stable than the S-capped monocyclic configuration, even though the two structures (linear and cyclic) are located very close to each other (5.6 kcal mol⁻¹). This effect is due to the high stability of the C_{18} entity present in the $C_{18}S$ cluster. Again the lowest energy isomers of $C_{19}S$ and $C_{20}S$ have a linear geometry in the ${}^1\Sigma^+$ and ${}^3\Sigma^-$ ground electronic states, respectively.

The rotational constants are found to agree satisfactorily with that estimated by experimental methods. We are thus confident that the method used (DFT/B3LYP) gives reliable prediction as for the structural parameters of medium-sized C_nS clusters. We hope that this study would stimulate further experimental determinations of these important quantities, especially the vibrational frequencies for which experimental information is still very fragmentary.

References

- [1] T. Kimura, T. Sugai, H. Shinohara, Chem. Phys. Lett. 256 (1996) 269.
- [2] J.L. Fye, M.F. Farrold, J. Chem. Phys. 101 (1997) 1836.
- [3] D.A. Williams, in: Molecules and Grains in Space, I. Nenner (Ed.), AIP Conference Proceedings No. 312, AIP New York 1994, p. 3.

- [4] B.E. Turner, in Chemistry and Spectroscopy of Interstellar Molecules, D. Bohme, E. Herbst, N. Kaifu, S. Saito (Eds.), University of Chicago Press, 1992, D. Bohme, p. 75.
- [5] H. Lavendy, J.M. Robbe, J.P. Flament, G. Pascoli, *J. Chim. Phys.* 94 (1997) 1779, and references therein.
- [6] G. Pascoli, H. Lavendy, *Int. J. Mass Spectrom. Ion Processes* 177 (1998) 31.
- [7] S. Saito, K. Kawaguchi, S. Yamamoto, M. Ohishi, H. Suzuki, N. Kaifu, *ApJ* 317 (1987) L115.
- [8] S. Yamamoto, S. Saito, K. Kawaguchi, N. Kaifu, H. Suzuki, M. Ohishi, *ApJ* 317 (1987) L119.
- [9] J. Cernicharo, M. Guelin, H. Hein, C. Kahane, *Astron. Astrophys.* 181 (1987) L9.
- [10] M.B. Bell, L.W. Avery, and P.A. Feldman, *ApJ* 417 (1993) L37.
- [11] D. Smith, N.G. Adams, K. Gilles, E. Herbst, *Astron. Astrophys.* 200 (1988) 191.
- [12] T.J. Millar, E. Herbst, *Astron. Astrophys.* 231 (1990) 231.
- [13] Y. Xie, H.F. Schaefer III, *J. Chem. Phys.* 96 (1992) 3714.
- [14] Z. Cai, X.G. Zhang, X.Y. Wang, *Chem. Phys. Lett.* 213 (1993) 168.
- [15] D.J. Peeso, D.W. Ewing, T.T. Curtis *Chem. Phys. Lett.* 166 (1990) 307.
- [16] A. Murakami, *ApJ* 410 (1993) L45.
- [17] S. Seeger, P. Botschwina, J. Flugge, H.P. Reisenauer, G. Maier, *J. Mol. Struct. (Theochem)* 303 (1994) 213.
- [18] S. Lee, *Chem. Phys. Lett.* 268 (1997) 69.
- [19] J.D. Presilla-Marquez, C.M.L. Rittby, W.R.M. Graham, *J. Chem. Phys.* 106 (1997) 8367.
- [20] M.L.J. Martin, J. El-Yazal, J.P. François, *Chem. Phys. Lett.* 242 (1995) 570.
- [21] W. Kohn, L.J. Sham, *Phys. Rev. A* 140 (1965) 1133.
- [22] A.D. Becke, *Phys. Rev. B* 45 (1992) 244.
- [23] A.D. Becke, *J. Chem. Phys.* 98 (1993) 5648.
- [24] C. Lee, W. Yang, R.G. Parr, *Phys. Rev. B* 37 (1988) 785.
- [25] R. Krishnan, J.S. Binkley, R. Seeger, J.A. Pople, *J. Chem. Phys.* 72 (1980) 650.
- [26] GAUSSIAN 94, Revision C.3, M.J. Frisch, G.M. Trucks, H.B. Schlegel, P.M.W. Gill, B.G. Johnson, M.A. Robb, J.R. Cheeseman, T. Keith, G.A. Petersson, J.A. Montgomery, K. Raghavachari, M.A. Al-Laham, V.G. Zakrzewski, J.V. Ortiz, J.B. Foresman, J. Cioslowski, B.B. Stefanov, A. Nanayakkara, M. Challacombe, C.Y. Peng, P.Y. Ayala, W. Chen, M.W. Wong, J.L. Andres, E.S. Replogle, R. Gomperts, R.L. Martin, D.J. Fox, J.S. Binkley, D.J. Defrees, J. Baker, J.P. Stewart, M. Head-gordon, C. Gonzalez and J.A. Pople, Gaussian, Inc., Pittsburgh, PA, (1995).
- [27] J. Hehre, L. Radon, P.V.R. Schleyer, J.A. Pople, *Ab Initio Molecular Orbital Theory*, Wiley, New York, 1982, p. 171.
- [28] Y. Hirahara, Y. Oshima, Y. Endo, *ApJ* 408 (1993) L113.
- [29] Y. Kasai, K. Obi, Y. Oshima, Y. Hirahara and Y. Endo, K. Kawagushi, A. Murakami *ApJ*. 410 (1993) L45.
- [30] P. Botschwina, S. Seeger, M. Horn, J. Flügge, M. Oswald, M. Mladenowic, U. Höper, R. Oswald, E. Schick, in *Molecules and Grains in Space*, I. Nenner, (Ed.), AIP Conference Proceedings No. 312, AIP New York, 1994, p. 321.
- [31] J. Bernholc and J.C. Phillips, *Phys. Rev. B* 33 (1986) 7395.
- [32] W. Weltner Jr., R.J. Van Zee, *Chem. Rev.* 89 (1989) 1713, and references therein.
- [33] P. Thaddeus, in *Molecules and Grains in Space*, I. Nenner (Ed.), AIP Conference Proceedings No. 312, AIP New York, 1994, p. 711.
- [34] B.T. Luke, J.A. Pople, M.B. Krogh-Jesperson, Y. Apeloig, M. Karni, J. Chandrasekhar, P.V.P. Schleyer, *J. Am. Chem. Soc.* 108 (1986) 270.
- [35] J.M. Hunter, J.L. Fye, E.J. Roskamp, M.F. Jarrold, in *Molecules and Grains in Space*, I. Nenner (Ed.), AIP Conference Proceedings No. 312, AIP, New York, 1994, p. 571.
- [36] N. Kurita, K. Kobayashi, H. Kunahora, K. Tato, K. Ozawa, *Chem. Phys. Lett.* 198 (1992) 95.
- [37] K. Ragavachari, J.S. Binkley, *J. Chem. Phys.* 87 (1987) 2191.
- [38] S. Fliszár, *Charge Distribution and Chemical Effects*, Springer Verlag, New York, 1983.
- [39] K.S. Pitzer, E. Clementi, *J. Am. Chem. Soc.* 81 (1959) 4477.